Study of jet quenching using photon-jet events in PbPb collisions at 2.76 TeV with CMS

Yue Shi Lai (for the CMS Collaboration)[1]

Laboratory of Nuclear Science, Massachusetts Institute of Technology, Cambridge, MA 02139-4301, USA

Abstract

The first measurement of the transverse momentum (p_T) imbalance of isolated-photon+jet pairs in relativistic heavy ion collisions is reported. The analysis uses data from PbPb collisions at a centre-of-mass energy of 2.76 TeV per nucleon pair, corresponding to an integrated luminosity of $150 \mu b^{-1}$ recorded by the CMS experiment at the LHC in 2011. For events containing an isolated photon with transverse momentum $p_T > 60$ GeV/c and an associated jet with $p_T > 30$ GeV/c, the photon+jet p_T imbalance is studied as a function of collision centrality and compared to pp data and PYTHIA calculations at the same centre-of-mass energy. Using the p_T of the isolated photon as an estimate of the energy of the scattered parton, this measurement allows an unbiased characterization of the in-medium parton energy loss.

1. Introduction

The interaction between energetic partons and the medium produced in relativistic heavy ion collisions has been previously studied at the LHC using dijets, where an enhanced asymmetry is observed compared to pp collisions [1, 2, 3]. While the study using dijets benefits from its large production rate, the energy loss of both partons complicates the inference of the amount of energy lost by each parton. Correlations between isolated photons and jets have been proposed in the literature as the "golden channel" to study jet energy loss, because the photon retains the kinematic information of the hard scattering [4, 5]. This article describes the first measurement of isolated-photon+jet correlations in $\sqrt{s_{NN}} = 2.76$ TeV pp and PbPb collisions with CMS [6].

2. Triggering and Photon/Jet Reconstruction

PbPb data with an integrated luminosity of $\int \mathcal{L} \, dt = 150 \, \mu b^{-1}$, and pp reference data with $\int \mathcal{L} \, dt = 231 \, nb^{-1}$, are used in this analysis. Events are recorded after passing the $p_T > 40$ GeV/c high level trigger in PbPb, and $p_T > 15$ GeV/c in pp.

The ECAL clustering algorithm and the algorithm to reject highly-ionizing particles described in [7] are used. The effect of the PbPb underlying event (UE) on the photon energy scale is corrected. Photons candidates with $p_T^\gamma > 60$ GeV/c in the barrel ECAL region of $|\eta^\gamma| < 1.44$ are used for further analysis, after removing any candidates within $|\Delta\eta| < 0.02$ and $|\Delta\phi| < 0.15$ of any
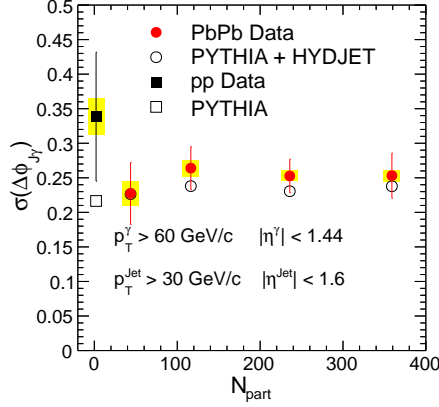

Figure 1: Fitted $\Delta\phi_{J\gamma}$ width (σ in Eq. (1), $\Delta\phi_{J\gamma} > \frac{2}{3}\pi$) between the photon and associated jet after background subtraction as a function of N_{part}. The error bars show the statistical uncertainty, and the yellow boxes indicate the systematic uncertainties.

electron tracks. Photon candidates with a hadronic-to-electromagnetic energy ratio $H/E < 0.1$ within $\Delta R = \sqrt{\Delta\eta^2 + \Delta\phi^2} = 0.15$ are clearly originating from neutral mesons, and are discarded [8]. Photon isolation is determined from the sum of track, hadronic calorimeter (HCAL) and ECAL energy within $\Delta R < 0.4$. This energy after subtracting the expected contribution from the UE forms the discriminant SumIso$^{\text{UE–sub}}$. The expected UE contribution is determined by averaging within the same η range. Compared to [7], a more stringent isolation threshold of SumIso$^{\text{UE–sub}} < 1$ GeV is applied to enhance the photon purity. The photon purity is determined in each centrality by a two component, template fit of the distribution of ECAL shower shape $\sigma_{\eta\eta}$, which is a modified second moment along the η direction. The signal distribution is derived from PYTHIA+HYDJET events and GEANT simulation, while the background enriched set of photon candidates with $10 < \text{SumIso}^{\text{UE–sub}} < 20$ GeV forms the background distribution. The signal photon is required to have $\sigma_{\eta\eta} < 0.01$. Residual contamination by decay photons in that range is removed statistically by applying the photon purity to the background template, where the purity ranges between 74–83%.

Jets are obtained by applying the anti-k_T clustering algorithm [10] and the distance parameter $R = 0.3$ on the particle-flow event reconstruction [9]. The UE energy is removed using the method described in [11]. After removing jets coinciding with the photon candidate within the distance parameter, all remaining jets with $p_T^{\text{Jet}} > 30\,\text{GeV}/c$ and within $|\eta^{\text{Jet}}| < 1.6$ are correlated with the photon candidates. Correlations with fake jets and multiple interaction are removed statistically, and additionally cross checked against a fake jet rejection discriminant.

The PbPb data is compared both to the pp data at the same $\sqrt{s_{NN}}$, and PYTHIA version 6.422 [12], tune Z2, embedded into the PbPb background events from HYDJET [13], and using GEANT simulation to determine the CMS detector response. The multiplicity, particle spectra, and elliptic flow obtained from HYDJET are tuned to reproduce the LHC PbPb data. The interaction between the high purity isolation with the PbPb UE is quoted as a systematic uncertainty, which is obtained by comparing the high purity SumIso $< 1\,\text{GeV}$ in PYTHIA+HYDJET and the generator level GenIso $< 5\,\text{GeV}$ isolation requirement without UE. The effect of a possible medium-modified jet fragmentation is studied by applying the analysis procedure using PYQUEN [13] photon+jets em-
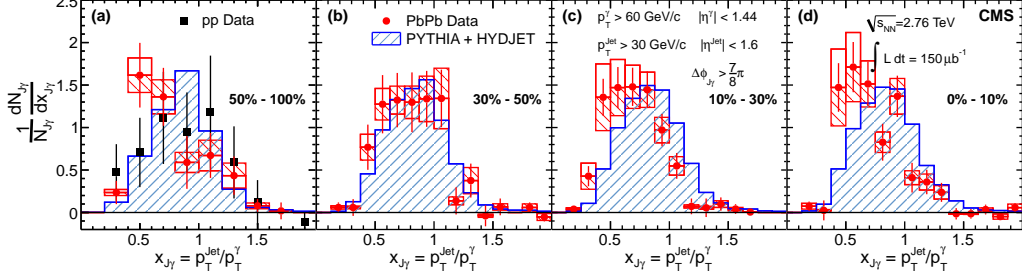
2

Figure 2: Distribution of the ratio between the photon ($p_T^\gamma > 60\,\mathrm{GeV}/c$) and jet ($p_T^{\mathrm{Jet}} > 30\,\mathrm{GeV}/c$, $\Delta\phi_{J\gamma} > \frac{7}{8}\pi$) momenta after subtracting background. The area of each distribution is normalized to unity. PbPb data (filled circles) are compared to the PYTHIA+HYDJET MC simulation (shaded histogram) and to pp data at $\sqrt{s} = 2.76\,\mathrm{TeV}$ (filled squares). The error bars on the points show the statistical uncertainty. See text for a description of the open/ shaded red systematic uncertainty boxes.

bedded into HYDJET, and the full analysis chain is found to extract the generator-level imbalance correctly.

3. Results

A possible modification of the photon+jet azimuthal decorrelation is studied using the unity-normalized $\Delta\phi_{J\gamma}$ distribution. The empirical parametrization by an exponential function

$$\frac{1}{N_{J\gamma}} \frac{dN_{J\gamma}}{d\Delta\phi_{J\gamma}} = \frac{e^{(\Delta\phi - \pi)/\sigma}}{(1 - e^{-\pi/\sigma})\,\sigma}, \tag{1}$$

with width σ is used to characterize the evolution of the width of the distribution as a function of N_{part}. Fig. 1 shows the aforementioned width parameter σ as a function of N_{part}. No significant change is observed between all PbPb centralities and with respect to pp data and PYTHIA tune Z2.

The ratio of jet p_T^{Jet} divided by the photon p_T^γ, $x_{J\gamma} = p_T^{\mathrm{Jet}}/p_T^\gamma$, is used to study the jet energy loss. Fig. 2 shows the unity-normalized $x_{J\gamma}$ distribution, again comparing the PbPb data in individual centrality bins to PYTHIA+HYDJET, and the 50–100% centrality bin also to pp data. The normalization induces a point-to-point anticorrelation in the systematic uncertainties. The signed systematic uncertainty is indicated by open and shaded uncertainty boxes, where the low/high x probability densities must balance. Fig. 3(a) shows the evolution of the distribution mean, $\langle x_{J\gamma} \rangle$, as function of N_{part}. A modest change in the $\langle x_{J\gamma} \rangle$ towards central collisions is observed, with a significant difference appearing between PbPb and PYTHIA tune Z2. However, the same comparison with pp data suffers from the large statistical uncertainty due to the small pp sample size, and remains rather marginal.

A complementary observation are jets losing sufficient energy to fall below the $p_T^{\mathrm{Jet}} > 30\,\mathrm{GeV}/c$ cut (the η distribution in PbPb is essentially identical to pp). The complementary observable to $\langle x_{J\gamma} \rangle$ is therefore the fraction of photons with an associated jet, $R_{J\gamma}$ Fig. 3(b) shows $R_{J\gamma}$ as a function of N_{part}. A significant decrease in the number of photons with an associated jet in central PbPb is observed.
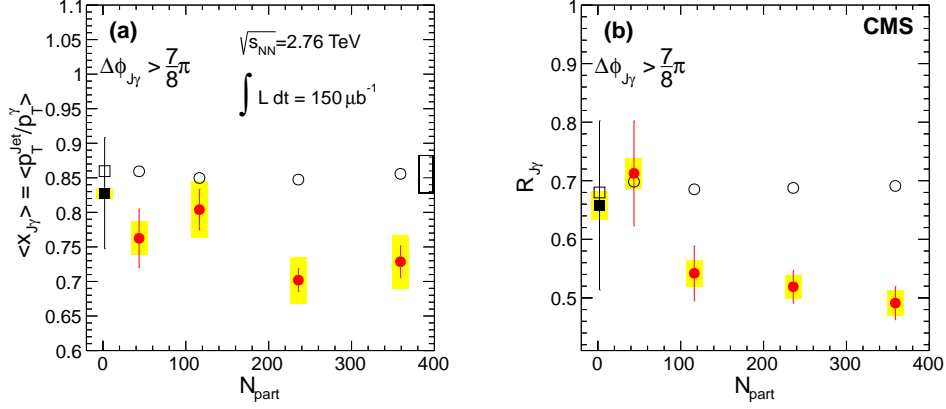
3

Figure 3: (a) Average ratio of jet transverse momentum to photon transverse momentum, $\langle x_{J\gamma} \rangle$, as a function of N_{part}. The empty box at the far right indicates the correlated systematic uncertainty. (b) Average fraction of isolated photons with an associated jet above $30\,\text{GeV}/c$, $R_{J\gamma}$, as a function of N_{part}. In both panels, the yellow boxes indicate point-to-point systematic uncertainties and the error bars denote the statistical uncertainty.

References

[1] S. Chatrchyan, et al., Observation and studies of jet quenching in PbPb collisions at $\sqrt{s_{NN}} = 2.76$ TeV, Phys. Rev. C 84 (2011) 024906. arXiv:1102.1957, doi:10.1103/PhysRevC.84.024906.

[2] G. Aad, et al., Observation of a centrality-dependent dijet asymmetry in lead-lead collisions at $\sqrt{s_{NN}} = 2.76$ TeV with the ATLAS detector at the LHC, Phys. Rev. Lett. 105 (2010) 252303. arXiv:1011.6182, doi:10.1103/PhysRevLett.105.252303.

[3] S. Chatrchyan, et al., Jet momentum dependence of jet quenching in PbPb collisions at $\sqrt{s_{NN}} = 2.76$ TeVSubmitted to *Phys. Lett. B*. arXiv:1202.5022.

[4] X.-N. Wang, Z. Huang, I. Sarcevic, Jet quenching in the direction opposite to a tagged photon in high-energy heavy-ion collisions, Phys. Rev. Lett. 77 (1996) 231. arXiv:9701227, doi:10.1103/PhysRevLett.77.231.

[5] X.-N. Wang, Z. Huang, Medium-induced parton energy loss in γ+jet events of high-energy heavy-ion collisions, Phys. Rev. C 55 (1997) 3047. arXiv:9605213, doi:10.1103/PhysRevC.55.3047.

[6] S. Chatrchyan, et al., The CMS experiment at the CERN LHC, JINST 03 (2008) S08004. doi:10.1088/1748-0221/3/08/S08004.

[7] S. Chatrchyan, et al., Measurement of isolated photon production in pp and PbPb collisions at $\sqrt{s_{NN}} = 2.76$ TeV, Phys. Lett. B 710 (2012) 256. doi:10.1016/j.physletb.2012.02.077.

[8] V. Khachatryan, et al., Measurement of the isolated prompt photon production cross section in pp collisions at $\sqrt{s} = 7$ TeV, Phys. Rev. Lett. 106 (2011) 082001. arXiv:1012.0799, doi:10.1103/PhysRevLett.106.082001.

[9] CMS Collaboration, Commissioning of the particle-flow reconstruction in minimum-bias and jet events from pp collisions at 7 TeV, CMS Physics Analysis Summary CMS-PAS-PFT-10-002 (2010).

[10] M. Cacciari, G. P. Salam, G. Soyez, The anti-k_t jet clustering algorithm, JHEP 04 (2008) 063. arXiv:0802.1189, doi:10.1088/1126-6708/2008/04/063.

[11] O. Kodolova, I. Vardanian, A. Nikitenko, A. Oulianov, The performance of the jet identification and reconstruction in heavy ions collisions with CMS detector, Eur. Phys. J. C 50 (2007) 117. doi:10.1140/epjc/s10052-007-0223-9.

[12] T. Sjöstrand, S. Mrenna, P. Z. Skands, PYTHIA 6.4 physics and manual, JHEP 05 (2006) 026. arXiv:hep-ph/0603175, doi:10.1088/1126-6708/2006/05/026.

[13] I. P. Lokhtin, A. M. Snigirev, A model of jet quenching in ultrarelativistic heavy ion collisions and high-p_T hadron spectra at RHIC, Eur. Phys. J. C 45 (2006) 211. arXiv:hep-ph/0506189, doi:10.1140/epjc/s2005-02426-3.